Published in final edited form as:
Exp Cell Res. 2010 August 1; 316(13): 2136–2151. doi:10.1016/j.yexcr.2010.04.017.

Recruitment of Uev1B to Hrs-containing endosomes and its effect on endosomal trafficking

Jason E. Duex, **Michael R. Mullins**, and **Alexander Sorkin**
Department of Pharmacology, University of Colorado Denver Medical School, Aurora, Colorado, USA

Abstract

Endocytosis of signaling receptors, such as epidermal growth factor receptor (EGFR), tightly controls the signal transduction process triggered by ligand activation of these receptors. To identify new regulators of the endocytic trafficking of EGFR an RNA interference screen was performed for genes involved in ubiquitin conjugation and down-regulation of EGFR. The screen revealed that small interfering RNAs (siRNAs) that target the conserved ubiquitin-binding domain Uev1 increased down-regulation of EGFR. Since these siRNAs simultaneously targeted multiple genes containing Uev1 domain, we analyzed the role of these gene products by overexpressing individual Uev1-related proteins. This analysis revealed that overexpression of Uev1A (UBE2V1) has no effect on the degradation of EGFR:EGF complexes. In contrast, overexpression of Uev1B (TMEM189-UBE2V1 isoform 2) slowed the degradation of EGF:receptor complexes. The Uev1B protein was found to strongly colocalize and associate with ubiquitin and Hrs in endosomes. Moreover, overexpression of Uev1B abrogated the ability of Hrs to colocalize with EGFR. The B-domain of Uev1B, and not the UEV-domain, was mainly responsible for the observed phenotypes suggesting the presence of a novel endosomal targeting sequence within the B-domain. Together, the data show that elevated levels of Uev1B protein in cells leads to decreased efficiency of endosomal sorting by associating with ubiquitinated proteins and Hrs.

Keywords

Uev1B; endosome; ubiquitin; EGFR; cell biology

INTRODUCTION

The endosomal system functions to sort various cellular molecules after their biosynthesis or endocytosis and deliver them to their proper intracellular destinations. While many of the key components in this system have been characterized, the molecular mechanisms controlling endosomal trafficking are not fully understood and there are a number of regulatory components which remain to be identified. Ultimately, a better understanding of endosomal sorting will shed light on the mechanisms underlying a variety of diseases such as those involving mysregulation of oncogenes, channels and transporters, viral infection and alterations in synaptic transmission.

Address correspondence to: Alexander Sorkin, Department of Pharmacology, University of Colorado Denver School of Medicine, Mail Stop F8303, PO Box 6511, Aurora, CO 80045 Tel: 303.724.3649; Fax: 303.724.3663 alexander.sorkin@ucdenver.edu.

One of the typical approaches to studying the endosomal system is to track a specific protein as it enters the system through endocytosis and follow its movement to the lysosome. A model protein used in many of these studies is the epidermal growth factor (EGF) receptor (EGFR). This receptor, when bound by ligand at the cell surface, induces an intracellular signal transduction process that promotes cell growth, differentiation, and survival. Normal cells terminate this signaling by trafficking the EGFR:ligand complexes through the endosomal system and sorting them for degradation in the lysosome in a process termed down-regulation [1]. Not surprisingly, inefficient down-regulation can lead to elevated levels of EGFR which is associated with many types of cancer.

The current models of EGFR down-regulation contend that upon ligand binding EGFR proteins are endocytosed, ubiquitinated, and internalized into early endosomes. Here the ligand-occupied EGFRs are bound by the Hrs (hepatocyte growth factor–regulated tyrosine kinase substrate) and STAM (signal transducing adaptor molecule) complex [2,3]. Upon binding to this Hrs/STAM complex, also known as $ESCRT_0$ (endosomal sorting complex required for transport), EGFR is incorporated into intralumenal vesicles of endosomes via a process of inward invagination of the limiting membrane of the endosome. This process is mediated by additional ESCRT complexes ($ESCRT_{I-III}$), each containing ubiquitin recognizing components. The incorporation of EGFR into intralumenal vesicles eliminates the ability of receptors to recycle and their ability to engage in the signaling pathway. These multivesicular endosomes eventually fuse with the lysosome where the contents are degraded in the proteolytic environment.

While the role of key proteins such as ubiquitin ligases and ESCRT components have been determined for down-regulating ubiquitinated cargo, more recent studies have identified a number of regulatory proteins which also play significant roles. For example, the deubiquitinase enzymes AMSH and UBPY (Usp8) have been shown to associate with ESCRTs and help control ubiquitination and sorting of receptors, such as EGFR [4-9], hepatocyte growth factor receptor (c-Met) [8,9], ErbB3 [8], protease activated receptor (PAR2) [10], and MHC class I molecules [5]. Additionally, AMSH and UBPY have been shown to regulate receptor trafficking by controlling ubiquitination of ESCRT proteins [6,9,11,12]. Similarly, modulating the levels of other Hrs associating proteins such as SCAMP3 [13] or Eps15b [14] have been shown to regulate EGFR trafficking. These studies suggest that there exists a complex framework regulating endosomal sorting and that a variety of peripheral proteins play significant roles. However, the extent of the framework is unknown and identifying all the proteins involved is critical to achieving a full understanding of the complex nature of endosomal sorting.

As an approach towards a better understanding of the endosomal sorting process, a RNAi screen was employed to further investigate the role of known endosomal sorting regulators and identify novel regulators. Reverse-transfection siRNA libraries were used and the knockdown of specific genes was analyzed for its ability to promote down-regulation of ubiquitinated cargo such as EGFR:ligand complexes [15,16]. One of the novel genes identified in this screen was Usp18. The corresponding protein has recently been demonstrated to be a potent regulator of EGFR cellular levels [16]. Additional analysis revealed that siRNA molecules targeting the Uev1A gene also demonstrated a significant effect on EGFR down-regulation. The Uev1A protein has a high degree of homology with E2 ubiquitin conjugating enzymes. However, the protein is catalytically inactive owing to the mutation of a catalytic cysteine residue [17]. Despite the inability of Uev1A to function on its own as a ubiquitin conjugase it does play a critical role in ubiquitin conjugation as a coeffector of Ubc13, an active E2 ubiquitin conjugase [18,19]. Closer analysis of the siRNA sequences targeting Uev1A revealed that they also target splice variants emanating from the Uev1 gene locus. Further studies involving the

overexpression of the various splice variants revealed a significant role for Uev1B in regulating the endosomal trafficking and sorting of EGFR.

MATERIALS AND METHODS

Cell culture and antibodies

University of Michigan squamous cell carcinoma (SCC2) cells were grown in DMEM (Gibco-Invitrogen, Carlsbad, CA) supplemented with 5% fetal bovine serum (FBS) (Hyclone, Logan, UT). COS1 and HeLa cells were grown in DMEM supplemented with 10% FBS. EGFR monoclonal antibodies (#528) used in the high throughput screen were purified from hybridoma cells - American Type Culture Collection (ATCC) (Manassas, VA). Antibodies used in western blot analysis included anti-EGFR (1005, Santa Cruz Biotechnology, Santa Cruz, CA), anti-transferrin receptor and anti-GFP (Zymed, San Fransisco, CA), anti-α-actinin (Cell Signaling, Danvers, MA), anti-actin and anti-ubiquitin (Sigma, St. Louis, MO). Antibodies used in supplemental data include anti-Hrs and anti-Vps24 (provided by Dr. H. Stenmark, Radium Institute, Oslo, Norway), anti-TGN46 (provided by Dr. G. Banting, University of Bristol, UK), anti-COP1 (Dr. I. Mellman, Genentech, CA), and anti-M6PR [20], anti-LAMP1 (H4A3, Santa Cruz Biotechnology), and anti-HA.11 (Covance, Emeryville, CA).

Plasmid constructs

Kua and Uev1A cDNA was kindly provided by Dr. Timothy Thomson (Barcelona Molecular Biology Institute, CSIC, Barcelona, Spain). Uev1B cDNA was kindly provided by Dr. Stanley Lin (Wesleyan University, Middletown, CT) with permission from Dr. Wei Xiao (University of Saskatchewan, Saskatoon, Saskatchewan). The cDNAs were cloned into pEYFP or pECFP vectors (Clontech, Mountain View, CA). The pYFP-KuaUev1B plasmid was generated by PCR amplifying the Kua gene using the forward CGAGCTCGTCGCCACCATGGCGGGCGCCGAGGACTGG and reverse AGCCTGTGGTGATGCAGAAG primers. The resulting PCR product was digested with Sac1- BsmBI and cloned into Sac1-BsmBI gapped pYFP-Uev1B. A stop codon was then added at the correct position using site directed mutagenesis. A pUev1B-YFP plasmid was generated by amplifying Uev1B with the forward CGAGCTCACCATGGCCTACAAGTTC and reverse GCCGCGGATTGCTGTAACACTG primers. The subsequent PCR product was digested and cloned into Sac1-SacII gapped EYFP-N3 vector. The pYFP-B-domain plasmid was generated by digesting pYFP-Uev1B with BsmBI-SmaI to remove the UEV-domain. The remaining vector fragment was treated with Klenow to fill in the 3’ overhang and re-ligated. The pYFP-UEV-domain plasmid was generated by PCR amplifying the UEV-domain from Uev1B using the forward TCCGAGCTCGGAGTAAAAGTCCCTCGC and reverse TACGCGCAGCGTGACCGCTACAC primers. The resulting UEV-domain PCR product was digested with Sac1-DraIII and cloned into Sac1-DraIII gapped pYFP-Uev1B. Generation of the EGFR-mRFP construct has been described previously [21]. GFP-Hrs was kindly provided by Dr. H. Stenmark (Radium Institute, Oslo, Norway). The preparation of CFP-Hrs and YFP-Hrs was described previously [22]. EGFR-mRFP construct is described in [23]. The pHA-Uev1B plasmid was generated by amplifying Uev1B from pYFP-Uev1B with the forward GTACGGGGTACCACCATGTACCCATACGATGTTCCAGATTACGCTGCCTACAAG TTC CGCACCCAC and reverse CATGCCTGTACATTAATTGCTGTAACACTGTCCTTCGG primers. The pUev1B-HA plasmid was similarly generated by amplifying Uev1B with the forward GTACGGGGTACCACCATGGCCTACAAGTTCCGCACCCACAC and reverse CATGCCTGTACATTAAGCGTAATCTGGAACATCGTATGGGTAATTGCTGTAACA CTG TCCTTCGG primers. Both PCR products were individually double digested with KpnI and BsrGI and cloned into KpnI-BsrGI gapped EYFP-N1 vector. The GST-Uev1B construct

was generated by digesting Uev1B-YFP with Eco47-3 and SmaI and ligating the product into SmaI gapped pGEX-6P-1.

DNA transfections

DNA transfections of pHA-Uev1B and pUev1B-HA were performed using the Lipofectamine2000 protocol (Invitrogen) with 2-3 μg DNA per 35mm dish. All other DNA transfections used the Effectene protocol (Qiagen, Valencia, CA) with 0.3-1.5 μg DNA per 35mm dish. Experiments were performed roughly 48 hrs after DNA transfection.

siRNA high throughput screen for EGFR levels

The screen has been described in detail previously [16]. Briefly, siRNA libraries targeting endocytosis [15] and ubiquitin-related genes were custom ordered (Catalog #G-004705-05, Dharmacon, LaFayette, Colorado) and received in 96-well format. SCC2 cultured cells were added to each well and the plates incubated at 37°C in 5% CO_2 for 72 hrs. One plate was left untreated while a sister plate was treated with 100 ng/ml EGF (ThermoFisher Scientific, Waltham, MA). Both plates were incubated at 37°C for 4 hrs. Cells were fixed and EGFR immunolabeling was carried out on the non-permeabilized cells followed by treatment with $G\alpha m^{HRP}$ (Jackson ImmunoResearch Laboratories, West Grove, PA) secondary antibody. Amplex Red hydrogen peroxidase assay solution (Molecular Probes, Eugene, OR) was added and the extent of HRP activity (indirect measurement of surface EGFR levels) was assessed for each well. The HRP signal in each well was normalized to cell number (CyQUANT, Molecular Probes) for each well. Normalized EGF-induced EGFR surface levels of non-targeting siRNA treated cells are shown as zero percent. Normalized EGFR surface levels of targeting siRNA treated cells are displayed as the percent decrease (lower surface EGFR levels) or increase (higher surface EGFR levels) from control, non-targeting siRNA treated cells.

Fluorescence microscopy

COS1 cells were transferred to coverslips coated with ECL Cell Attachment Matrix (Millipore, Billerica, MA) 24 hrs after DNA transfection. After an additional 24 hrs coverslips were viewed at room temperature for single plane experiments with the exception of dextran experiments. COS1 cells were pulse-labeled in serum-free DMEM with 2mg/ml dextran-TexasRed (10,000 MW, lysine fixable (Invitrogen)) for 15 min at 37°C in 5% CO_2. The cells were then moved to room temperature in 5% CO_2 for 2 hours followed by PBS wash and fixation in 4% paraformaldehyde (Electron Microscopy Sciences, Hatfield, PA). Coverslips were then mounted onto slides with Mowiol (Invitrogen). All images were acquired using a Mariannas Imaging system consisting of a Zeiss inverted microscope equipped with a cooled CCD CoolSnap HQ (Roper, CA), dual filter wheels and a Xenon 175 W light source, all controlled by SlideBook software (Intelligent Imaging Innovations, Denver, CO). Image analysis was performed using the SlideBook 4 software.

Quantification of EGF-Rh degradation

COS1 cells were transfected with various DNA constructs and cells transferred to coverslips 24 hrs later. After an additional 24 hrs, the cells were placed on ice and 40 ng/ml EGF-Rhodamine conjugate (Molecular Probes) was added to the media to allow for binding to surface EGFR. Following 45 min incubation on ice fresh media was added and the cells incubated at 37°C for either 5 min or 2 hrs to allow for internalization and degradation of EGFR:EGF-Rh complexes, respectively. Cells were then washed 1x with PBS (pH 7.4) and fixed at room temperature with 4% freshly-prepared paraformaldehyde in Ca^{2+}/Mg^{2+}-free PBS for 15 min. For each coverslip images (z-stacks of 20 optical sections) of individual cells expressing a YFP construct were captured with both CY3 (EGF-Rh signal) and YFP filters (minimum 30 cells). Additionally, for each coverslip z-stacks of images of individual cells not

expressing a YFP construct were captured (minimum 30 cells). Total cellular CY3 or YFP signals were quantitated using the SlideBook 4 software. For each coverslip the percent difference between cells expressing a YFP construct and those not expressing a YFP construct was calculated. This percent difference for each coverslip was then normalized so the coverslips expressing YFP-alone was zero. Each construct was analyzed in at least three independent experiments.

siRNA transfections

Transfections were performed on SCC2 cells with the standard Dharmacon protocol using Dharmafect2 reagent and the appropriate oligonucleotide (25 or 50nM). The transfection was repeated after 24 hrs and cells were lysed at 72 hrs in TGH buffer as described previously [16]. Western blot analysis was carried out using specific antibodies detailed above. All RNAi oligonucleotides were from Dharmacon and included Non-targeting #2, B-domain #1 (GAGACCUACUUCUGCAUCAUU (#D-032200-13)), and B-domain #3 (CACGUAAACACCAUCGCAUUU (#D-032200-15)).

FRET measurements

The method of sensitized FRET measurements used to examine FRET between CFP and YFP has been described previously [21,23]. Briefly, images through YFP, CFP, and FRET filter channels were acquired using a Mariannas™ fluorescence imaging workstation. Images were background-subtracted and the corrected FRET ($FRET^C$) was calculated. $FRET^C$ images were presented in a quantitative pseudocolor. All calculations were performed using the FRET statistic module of SlideBook 4.0 or 4.1.

GST pull-down

The pGEX-6P-1 and pGEX-6P-Uev1B plasmids were transformed into BL21-DE3 cells. Cultures were grown for 4 hrs at 37°C in the presence of ampicillin and 0.3 mM IPTG. Pelleted cells were resuspended in TE (10 mM Tris, pH 8.0, 1 mM EDTA, 1 mM PMSF), sonicated, and incubated at 4°C for 30 min after the addition of sarkosyl (0.5% final). Following a spin at 20,000 × g the supernatant was added to pre-washed glutathione-sepharose beads (GE Healthcare) and incubated for 30 min at room temperature. HeLa cell extracts (TGH lysis buffer as described previously [16]) were incubated with GST-fusion precipitates for 2 hr at 4°C followed by washing with TGH, SDS-PAGE, and transfer to nitrocellulose. The blot was incubated with Ponceau S (Pierce, Rockford, IL) and imaged. Following washes the blot was probed with Hrs and ubiquitin antibodies.

RESULTS

siRNA targeting Uev1A promotes EGFR down-regulation

In an attempt to identify novel proteins that regulate the trafficking of ubiquitinated cargoes a RNAi screen was employed. This screen used siRNA libraries and a recently developed “in cell western blot” assay [16] to quantitatively assess the surface levels of EGFR following depletion of specific genes. Human squamous cell carcinoma cells (SCC2) were used in initial studies because they have very high levels of EGFR and are growth-dependent on the receptor [24]. The siRNA library screening experiments showed that treatment of cells for 72h with siRNA targeting Uev1A resulted in a 20% and 65% reduction in the amount of EGFR at the surface of cells untreated and treated with EGF, respectively (Figure 1A). Quite surprisingly, treatment of SCC2 cells with siRNA targeting Ubc13, the enzymatically active coeffector of Uev1A, had no significant effect on EGFR levels in this screen (Figure 1A). Similarly, siRNA targeting Mms2, which is also a coeffector of Ubc13 [25,26], had no significant effect on EGFR

levels (Figure 1A). These results collectively suggest a unique function for Uev1A in EGFR regulation, one that is independent from its role as a coeffector with Ubc13.

Analysis of the target sequences for the Uev1A siRNA oligonucleotides (pool of four) revealed that they targeted the UEV-domain of Uev1A (Figure 1B). Such targeting, however, means that they also inhibit expression of other gene transcripts which contain the UEV-domain. In humans the transcripts Kua (TMEM189), KuaUev1B (TMEM189-UBE2V1 isoform 1), Uev1B (TMEM189-UBE2V1 isoform 2; CROC-1B), and Uev1A (UBE2V1; CROC-1A) are produced from a gene locus that is the result of an evolutionary gene fusion event between the Uev1A and Kua genes [27,28]. This fusion event is also present in rhesus monkey and chimpanzee genomes (Figure 1C). However, it is not evident in the mouse genome (Figure 1C), nor any lower species (data not shown). Despite the absence of the fusion event outside of primates it is important to realize that each of the domains found in these proteins is conserved from nematodes to humans.

Subcellular localization of Uev1A-related proteins

While these initial RNAi studies demonstrated that siRNA oligonucleotides targeting the UEV-domain had a significant effect on EGFR protein levels, they could not delineate which gene product(s) is responsible. In fact, further analysis of these four gene transcripts using a RNAi approach would be inefficient due to the large expanse of identical sequences. Therefore, subsequent analyses were conducted with overexpression of individual constructs. Constructs were generated as YFP-fusions to allow for expression confirmation and potential localization studies (in lieu of the lack of effective Uev1 or Kua antibodies). Six different constructs were made including the four known gene products and two of the highly conserved domains. The expression and localization of the corresponding gene products were tested in COS1 cells. These cells were chosen because, unlike SCC2 cells, they have an ability to efficiently express exogenous DNA and have a superior morphology for analysis by microscope.

YFP-Kua and YFP-KuaUev1B proteins exhibited a predominantly endoplasmic reticulum (ER) pattern of localization (Figure 2). Some nuclear staining and a few punctae in the perinuclear region were also observed. These observations in living cells are consistent with previous studies in which the cellular distribution of Kua and KuaUev1B were investigated using small-epitope-tagged constructs by immunofluorescence [28]. Furthermore, the membrane localization is consistent with the prediction that Kua and KuaUev1B have 3 transmembrane domains (Figure 2).

The YFP-Uev1B protein, despite sharing 2 of 3 domains with KuaUev1B (Figure 1B), exhibited a markedly different distribution (Figure 2). The protein displayed a diffuse, cytoplasmic distribution with no ER morphology and no nuclear staining. In addition, YFP-Uev1B accumulated in distinct punctae that were found dispersed throughout the cytosol. This same cellular distribution was observed with Uev1B tagged with the small hemagglutinin (HA) epitope tag (Uev1B-HA and HA-Uev1B) suggesting that the punctate pattern of localization of Uev1B is not due to the attachment of a large protein such as YFP (Figure S1A). While the punctae suggest a degree of membrane association it is less than the Kua or KuaUev1B proteins. This reduced membrane localization is consistent with the loss of 2 of 3 transmembrane regions predicted for Kua or KuaUev1B proteins (Figure 2). In fact, due to the highly soluble appearance of the YFP-Uev1B protein it seems likely that the remaining putative transmembrane domain is not functional in that capacity. When only the B-domain is expressed as a YFP-fusion, it displayed a distribution that is very similar to that of Uev1B (Figure 2). However, there were generally fewer cytosolic punctae. The strong similarity in localization between Uev1B and B-domain suggests that the B-domain plays a significant role in localizing Uev1B to intracellular membranes, and perhaps a lesser role for localizing Kua and KuaUev1B.

Analysis of YFP-Uev1A localization revealed the protein localized mostly to the nucleus with lower levels distributed diffusely throughout the cytoplasm (Figure 2). Such an observation is consistent with reported localization of small-epitope-tagged Uev1A [18,28]. Interestingly, localization of YFP-UEV-domain appeared to be identical to that of Uev1A. The two proteins differ by just 30 amino acids at the N-terminus. Therefore, it appears this N-terminal sequence of Uev1A plays no significant role in its localization.

Additional studies of all six proteins revealed that N-terminal and C-terminal YFP fusions displayed identical phenotypes (data not shown). Taken together, all six proteins exhibited some form of cytosolic distribution but it remains to be determined which of the variants have an ability to regulate ubiquitinated cargo.

The Uev1B splice variant inhibits EGF down-regulation

The initial RNAi experiments suggested that depletion of KuaUev1B, Uev1B, and/or Uev1A from cells leads to increased trafficking of ubiquitinated cargo such as EGFR:ligand complexes. To help determine which of these proteins actually play a role the newly characterized YFP-fusions were overexpressed in COS1 cells and the extent to which internalized EGFR ligand (EGF) was degraded was assessed. EGF and EGFR do not significantly dissociate in endosomes and thus measuring the internalized levels of EGF is a viable means of measuring internalized EGFR [29]. Cells overexpressing individual YFP-fusion constructs were incubated on ice with EGF conjugated to rhodamine (EGF-Rh). Then, after 2 hrs at 37°C the amount of fluorescent ligand remaining in the cell was determined by microscopy using single cell quantitation. These studies revealed that, relative to control cells overexpressing YFP, overexpression of YFP-Uev1B resulted in a 140% increase in EGF-Rh signal remaining after 2 hrs incubation, indicative of a reduced rate of EGFR degradation (Figure 3A). The cellular distribution of EGF-Rh also appeared to be affected by Uev1B overexpression. Cells not expressing YFP-Uev1B showed that EGF-Rh was located mostly in the juxta-Golgi area while cells overexpressing YFP-Uev1B caused strong accumulation of EGF-Rh in vesicular compartments (presumably endosomes) in the perinuclear and peripheral areas of the cell (Figure 3B). Similar to Uev1B, overexpression of YFP-B-domain resulted in a 67% increase in EGF-Rh signal (Figure 3A). Overexpression of YFP-KuaUev1B and YFP-Kua, other B-domain-containing proteins, had small effects on EGF-Rh degradation (19% and 11%, respectively) which were not statistically significant (Figure 3A). YFP-Uev1A and YFP-UEV-domain expression had no effect on EGF-Rh degradation (Figure 3A), supporting the notion that the B-domain has the major role in the inhibitory effect of Uev1B on EGFR degradation.

While the increased amount of EGF-Rh observed in Uev1B overexpressing cells was likely the result of slow lysosomal targeting and degradation of EGFR:EGF-Rh complexes, it is also possible that the higher levels of EGF-Rh in Uev1B overexpressing cells is due to accelerated EGFR:EGF-Rh internalization. To investigate this possibility the EGF-Rh signal was measured after cells were chased at 37°C for only 5 min. With a 5 min chase the amount of endosomal EGF-Rh is determined predominantly by the rates of internalization. As shown in Figure 3C, cells overexpressing YFP-Uev1B had the same amount of internalized EGF-Rh after 5 min as control cells on the same coverslip not expressing YFP-Uev1B. Again, after 2 hrs cells overexpressing YFP-Uev1B had a significantly increased level of EGF-Rh relative to control cells. Thus, Uev1B overexpression does not appear to significantly affect EGF-Rh binding or endocytosis. Taken together, these data suggest that Uev1B, and to a lesser extent the B-domain alone, inhibits the degradation of endocytosed EGFR.

The observation that elevated levels of Uev1B slow EGFR down-regulation suggests that siRNA depletion of Uev1B may augment EGFR down-regulation. As stated above, UEV-domain targeted siRNA duplexes used in the screen (Figure 1A) would deplete all species

containing the UEV domain. Therefore, to increase the specificity of siRNAs towards targeting only species containing the B-domain, several siRNA targeting B-domain sequences were obtained. Treatment of SCC2 cells with either of two different B-domain siRNA duplexes resulted in a roughly 50% decrease in the EGFR level, even in the absence of ligand (Figure 3D). Both oligonucleotides each show strong specificity for blocking the expression of YFP-Uev1B (Figure 3E). This RNAi data is consistent with the UEV-domain RNAi data (Figure 1A) which also targeted Uev1B. In both cases, treatment of cells with RNAi directed towards Uev1B lead to a significant down-regulation of EGFR. Furthermore, the observation that depleted levels of Uev1B promote EGFR down-regulation is entirely consistent with the observation that increased levels of Uev1B inhibit EGFR down-regulation.

Uev1B localizes to endosomes but does not colocalize with internalized EGF or EGFR

The cytosolic punctate distribution of YFP-Uev1B suggests vesicular or endosomal localization. To investigate this possibility COS1 cells expressing YFP-Uev1B were incubated with dextran conjugated to the Texas Red (TxR) fluorophore. This fluid phase marker is taken up by cells through endocytosis and accumulates in early and late endosomal compartments. Significant colocalization between YFP-Uev1B punctae and dextran-TxR-positive structures was observed (Figure 4A). In some cells YFP-Uev1B exhibited a very high degree of colocalization with dextran while other cells had only a few endosomes containing YFP-Uev1B. These data suggest the endosomal nature of YFP-Uev1B structures. However, none of the specific early, late, and recycling endosome protein markers yielded significant colocalization with Uev1B (Table S1). Similarly, protein markers for organelles such as Golgi apparatus and endoplasmic reticulum exhibited no colocalization with Uev1B. Altogether, fluorescence microscopy analysis suggests that the punctae of Uev1B represents a specific subset of endosomal compartments.

The localization of YFP-Uev1B to endosomes, and its ability to regulate EGFR down-regulation, suggests that the two proteins may associate in endosomes. Therefore, localization of EGF:EGFR complexes and YFP-Uev1B was compared. COS1 cells expressing YFP-Uev1B were treated continuously with EGF-Rh for 15 min and analyzed by microscopy. YFP-Uev1B exhibited a diffuse cytosolic and vesicular-like punctate distribution after ligand treatment (Figure 4B and C). Interestingly, the YFP-Uev1B signal in some cells was seen in compartments displaying a “doughnut-like” morphology, characteristic of large endosomes. Similarly, EGF-Rh displays both a diffuse (plasma membrane) and punctate cytosolic distribution (endosomes) (Figure 4B). However, despite these similarities in intracellular distribution, colocalization between YFP-Uev1B and EGF-Rh was not observed. In fact, no colocalization was observed during 5-75 min of cell incubation with EGF-Rh (data not shown). These same observations were made in cells co-expressing YFP-Uev1B and EGFR-mRFP (Figure 4C). These localization experiments and the functional experiments detailed above suggest that Uev1B and EGFR:ligand complexes exist on similar intracellular structures. However, Uev1B regulates EGFR:ligand complexes not by directly interacting with them but likely through intermediary processes.

Uev1B associates with endosomal ubiquitin and suppresses the CFP-ubiquitin-induced “enlarged-endosome” phenotype

Uev1B contains a UEV ubiquitin-binding domain and may associate with ubiquitinated cargo or ubiquitinated sorting machinery. Therefore, as a first step towards elucidating the mechanism of Uev1B regulation of EGFR:ligand complexes we decided to test for colocalization between YFP-Uev1B and CFP-ubiquitin. When CFP-ubiquitin alone was overexpressed, it was localized in the nucleus, cytosol, and on the limiting membrane of endosomes (Figure 5A). Interestingly, CFP-ubiquitin overexpression caused a dramatic enlargement of endosomes (Figure 5A). Such an “enlarged-endosome” phenotype appeared to

be suppressed when CFP-ubiquitin is co-expressed with YFP-Uev1B (Figure 5B,C). Moreover, overexpressed CFP-tagged ubiquitin strongly colocalizes with Uev1B in endosome-like vesicular structures which were of a small size (Figure 5B).

To investigate whether Uev1B and ubiquitin may directly associate, sensitized fluorescence resonance energy transfer (FRET) microscopy was employed. The FRET analysis revealed that the punctae of YFP-Uev1B and CFP-ubiquitin exhibited strong corrected FRET ($FRET^C$) signals (Figure 5B). The high degree of colocalization and FRET between Uev1B and ubiquitin strongly suggests that these two overexpressed proteins are in close proximity and possibly interact in the cell. Perhaps this association allows Uev1B to regulate trafficking of ubiquitinated cargo (e.g., EGFR) or interfere with the function of ubiquitinated sorting proteins on endosomes, such as components of the ESCRT system.

The localization of YFP-B-domain was quite similar to that of YFP-Uev1B (Figure 2). Consistent with this observation the YFP-B-domain also displayed strong colocalization with CFP-ubiquitin (Figure 5A) and also suppressed the “enlarged-endosome” phenotype (Figure 5C). Furthermore, YFP-B-domain also exhibited FRET with CFP-ubiquitin, although the relative values of $FRET^C$ were lower than the values measured for the YFP-Uev1B:CFP-ubiqutin FRET pairing (data not shown). This observation suggests that the B-domain of Uev1B, and not the UEV-domain, is primarily responsible for associating with ubiquitin.

Overexpression of YFP-Kua or YFP-KuaUev1B also suppressed the “enlarged-endosome” phenotype, although to a lesser degree than Uev1B or B-domain (Figure 5C). By contrast, YFP-Uev1A or YFP-UEV-domain had an insignificant effect on the CFP-ubiquitin induced endosomal morphology as compared with endosomes in control cells expressing YFP alone. Thus, quantitative analysis of many images of cells co-expressing CFP-ubiquitin and YFP-tagged fusion proteins demonstrated that all proteins which contain the B-domain have the ability to suppress the CFP-ubiquitin-induced “enlarged-endosome” phenotype and promote a “small-endosome” phenotype (Figure 5C).

Uev1B colocalizes and associates with cytosolic Hrs

To further elucidate the nature of Uev1B containing vesicular structures in relation to the endosomal proteins involved in EGFR sorting, the localization of YFP-Uev1B was compared to that of transiently expressed CFP-Hrs, a protein that binds ubiquitinated cargo like EGFR in endosomes. Surprisingly, YFP-Uev1B was highly colocalized with CFP-Hrs in endosomes (Figure 6A). Additionally, CFP-Hrs displayed the same extent of colocalization with HA-Uev1B, suggesting that such colocalization is not due to YFP attached to Uev1B (Figure S1B). The overexpression of CFP-Hrs leads to “swelling” of endosomes, and in cells co-expressing both fusion proteins, many large endosomes were decorated with both CFP-Hrs and YFP-Uev1B (Figure 6A). It should be noted that the ratio of endosomal to cytosolic YFP-Uev1B signal shifts significantly to the former when Hrs is overexpressed. This suggests that Hrs recruits Uev1B to endosomes and that these two proteins may interact on endosomal membranes. Such an interaction is strongly supported by the observation of FRET between YFP-Uev1B and CFP-Hrs (Figure 6A). Furthermore, as with all previous comparative experiments above, the YFP-B-domain protein exhibited very similar phenotypes to that of YFP-Uev1B (Figure 6B).

Additional evidence for interaction between Uev1B and Hrs was obtained in GST pull-down experiments. Recombinant GST-Uev1B or GST alone was incubated with HeLa cell extracts and precipitated proteins were analyzed by western blotting. As shown in Figure 6C Hrs was detected specifically in GST-Uev1B pull-downs (Figure 6C). Furthermore, GST-Uev1B was also able to precipitate ubiquitinated proteins (Figure 6C). These observations are consistent

with the colocalization of two proteins and the FRET data, and strongly suggest that Uev1B interacts with Hrs and ubiquitinated proteins in endosomes.

Uev1B interferes with EGF-Rh colocalization with Hrs

Hrs is a component of the ESCRT system responsible for sorting of internalized, ubiquitinated cargo (e.g., EGFR) to the lysosome for degradation. Hrs has been shown to colocalize with internalized EGFR and EGF [30-32]. Since previous experiments demonstrated that Uev1B associates with heterologously-expressed Hrs and also affects trafficking of internalized EGFR:ligand complexes, the relative localization of all three proteins was analyzed. Cells expressing CFP-Uev1B and YFP-Hrs were treated with EGF-Rh for 20 min at 37°C. Microscopic analysis demonstrated that CFP-Uev1B strongly colocalized with YFP-Hrs and that YFP-Hrs colocalized with EGF-Rh (Figure 7A). However, no significant colocalization of all three proteins was observed. Moreover, in individual cells expressing both CFP-Uev1B and YFP-Hrs, very little colocalization between YFP-Hrs and EGF-Rh was observed, whereas CFP-Uev1B and YFP-Hrs were highly colocalized (Figure 7B and C). In contrast, in cells expressing only YFP-Hrs, there was a very high degree of colocalization between YFP-Hrs and EGF-Rh (Figure 7D). Taken together, these observations suggest that in the presence of Uev1B, Hrs is precluded from colocalization and association with EGFR. Such a model is consistent with the ability of Uev1B to inhibit down-regulation of EGFR. Therefore, it is plausible to suggest that Uev1B competitively associates with Hrs, limiting the ability of Hrs to properly sort ubiquitinated cargo for degradation in the lysosome (Figure 7E).

DISSCUSSION

We characterized the effects on endosomal trafficking of each of the 4 proteins derived from the human Uev1 gene locus. These experiments revealed that the Uev1B protein plays a significant role in regulating the intracellular trafficking of internalized EGFR. Furthermore, first time analysis of the intracellular distribution of Uev1B revealed that the protein is excluded from the nucleus and forms multiple cytosolic punctae. In contrast, the cellular distribution of the other 3 proteins was found in these studies to be either predominantly nuclear (Uev1A) or predominantly ER associated (Kua and KuaUev1B). Importantly, the studies presented here using YFP-fusion proteins of these other 3 proteins fully support those observations made previously with HA-tagged proteins [28]. Thus, it appears that among the 4 proteins originating from the Uev1 gene locus only Uev1B has a predominately cytosolic cellular distribution. Interestingly, overexpression of Uev1B also had the greatest inhibitory effect on EGFR down-regulation.

The cytosolic punctae observed with Uev1B overexpression suggest that Uev1B proteins localize to specific cytosolic membrane compartments. The uniform dispersal of the punctae throughout the cytosol and their presence in both low and high expressing cells strongly argues against the notion that the punctae are merely cytosolic aggregates. The endosomal nature of Uev1B compartments is demonstrated by accumulation of endocytosed fluorescent dextran in these compartments under conditions when traffic to lysosomes is inhibited by low temperature. Additionally, YFP-Uev1B was sometimes seen associated with the “doughnut-shape” compartments characteristic of large endosomes. Furthermore, Uev1B was highly colocalized with overexpressed Hrs in endosomes, which confirms that Uev1B is indeed capable of association with the endosomal membrane. Surprisingly, however, Uev1B punctae did not colocalize with CFP-fusions of resident endosomal proteins such as Rab5, Rab7, and Rab11 (Table S1). Similarly, Uev1B did not colocalize with Lysotracker or markers of the ER/Golgi system (Table S1). It remains a distinct possibility that a specific colocalization marker has not yet been identified. Alternatively, a specific stimulus may be lacking in these studies which would promote colocalization of the punctae with a known organelle marker. Finally, it is possible that overexpression of Uev1B creates unique structures that have previously not

been identified. Additional characterization of these structures will be important in more precisely determining the mechanism by which Uev1B affects trafficking of EGFR.

Despite the strong ability of overexpressed Uev1B to inhibit EGFR trafficking the Uev1B punctae structures did not colocalize with internalized EGFR or its ligand. Such an observation suggests that Uev1B does not act directly upon internalized EGFR. The more likely scenario is that Uev1B acts in concert with other proteins which help control endosomal sorting of internalized cargo. One of these potential proteins is ubiquitin. Cells in which ubiquitin is fused with CFP or other fluorescent proteins (FPs) and overexpressed often display large endosomes decorated with FP-ubiquitin, similar to the cells with overexpressed Hrs [32,33]. This suggests that FP-ubiquitin interferes with normal trafficking of ubiquitinated cargo through endosomes and/or with normal function of the ubiquitinated ESCRT components. This could be related to aberrant ubiquitination and/or deubiquitination of endosomal substrates by FP-ubiquitin. It is unlikely to be due to the presence of unconjugated FP-ubiquitin because the mutant version of FP-ubiquitin (GG/AA mutant), which is incapable of substrate conjugation, was not detected in endosomes or found to cause any change in endosome morphology [34]. Likewise, strong recruitment of CFP-ubiquitin mutants K63R and K48R to endosomes along with their ability to produce the “enlarged-endosome” phenotype (data not shown) indicates that the behavior of FP-ubiquitin is unlikely due to inability of FP-ubiquitin to form K63- and K48-linked ubiquitin chains. The observations presented here demonstrated the ability of Uev1B to associate with ubiquitinated proteins (Figure 6C) and CFP-ubiquitin, causing a shift from an “enlarged-endosome” phenotype to a “small-endosome” phenotype (Figure 5). Such observations strongly suggest that Uev1B has the capacity to associate with and control the ability of ubiquitin to regulate endosome function.

The observation that Uev1B can associate with ubiquitin is at first not too surprising. The protein contains a UEV domain. The UEV domain of Tsg101 has affinity, albeit weak (mM), for ubiquitin moieties [35,36]. However, what is surprising is the fact that the B-domain by itself behaves almost identically to Uev1B. Furthermore, the UEV-domain alone showed neither colocalization with ubiquitin nor an ability to suppress the ubiquitin-induced “enlarged-endosome” phenotype. In addition, the B-domain-containing proteins Kua and KuaUev1B both display small degrees of colocalization with CFP-ubiquitin and an ability to suppress the “enlarged-endosome” phenotype. These observations strongly suggest that it is the B-domain of Uev1B that is mainly responsible for ubiquitin and endosome association, whereas the UEV-domain may additionally stabilize the interactions of Uev1B with endosomal proteins.

Analysis of the short 83 amino acid sequence of the B-domain revealed very few conserved sequences. However, one sequence of note was a conserved YXXL motif (where X is any amino acid residue), a classical internalization motif that binds to μ subunits of clathrin adaptor complexes [37]. A tyrosine phosphorylated form of the same peptide is known to associate with SH2 domains [38-40]. Therefore, it is possible that the $Y^{43}XXL^{46}$ motif found in the B-domain of Uev1B is required for association with SH2 domain containing proteins and/or components of the endomembrane system. However, mutation of the motif in Uev1B to FXXL or AXXA caused no significant change in cellular localization (data not shown). Thus, this motif is not involved in targeting of Uev1B to components of the endomembrane system.

Another protein found to colocalize and associate with Uev1B is the $ESCRT_0$ component Hrs, a main player in the sorting of ubiquitinated cargo. Both knock-down and overexpression of Hrs leads to inhibition of EGFR down-regulation [41,42]. Overexpression of Hrs is known to cause recruitment of other proteins that normally do not colocalize with Hrs, into large Hrs-containing endosomes [41-43]. Such observations demonstrate that it is critical for the cell to maintain the proper levels of Hrs in order to efficiently sort internalized EGFR:ligand complexes for degradation. The studies presented here demonstrate that overexpressed Uev1B

colocalizes with and is located in very close proximity to Hrs (FRET analysis). In addition, the predominantly cytoplasmic distribution of Uev1B becomes predominantly membrane-bound when higher levels of Hrs are present. Lastly, recombinant Uev1B is able to pull Hrs from cellular extracts. Thus, there appears to be a strong association between Uev1B and Hrs. Perhaps in normal cells Uev1B levels are low and Hrs is mostly free to perform its critical sorting functions at the sorting endosomes. However, higher levels of Uev1B may lead to an increase in Uev1B-Hrs complexes, resulting in a significant decrease in the sorting efficiency of EGFR:ligand complexes for degradation (Figure 7E). Such a model is supported by the studies presented here showing that in cells overexpressing Uev1B there is a dramatic decrease in colocalization between Hrs and EGFR:ligand complexes. Thus, it seems quite likely that increased levels of Uev1B in cells can abolish Hrs function.

While the levels of Uev1B mRNA in cells tested to date are considered low it is also important to realize that expression of Uev1B protein may not originate from a unique mRNA but rather from an internal ribosomal entry site on the KuaUev1B mRNA. Thus, it remains to be determined precisely how the Uev1B protein is generated and the extent to which it may be elevated in cancerous tissues. Interestingly, the levels of KuaUev1B mRNA are dramatically higher in SK-N-SH neuroblastoma, SK-PC-1 pancreatic cancer [28], and T24 bladder cancer cells lines relative to most cell lines (e.g., HeLa) tested (data not shown). In addition, transcripts encoding the UEV domain of Uev1A, Uev1B, and KuaUev1B were found to be up-regulated in human tumor-derived cell lines [44]. Of further interest is data from a study which established a cDNA library of tumor antigenic clones derived from Panc-1 cells and a patient with colon cancer [45]. A fragment of the Kua gene was among the cDNA clones generated. Furthermore, expression of Kua or B-domain peptides elicited the largest immune response from cytotoxic T lymphocytes suggesting that these proteins may represent biomarkers and/or targets for immunotherapy.

Importantly, our studies also demonstrated that cells expressing significant amounts of Uev1B would have reduced efficiencies for down-regulating EGFR and, therefore, a higher propensity for uncontrolled cell growth. It is also important to note that the Kua protein, which contains the B-domain, is not unique to primates as KuaUev1B and Uev1B are. Thus, functions associated with Kua and/or the B-domain may be conserved throughout all eukaryotes.

In summary, analysis of proteins emanating from the Uev1 locus in humans revealed that the Uev1B splice variant plays a role in endomembrane trafficking. These studies found that the protein relies predominantly on its B-domain to associate with endosomal components such as Hrs and endosome-associated ubiquitin, allowing it to play a role in regulating trafficking of cargo such as EGFR. It is quite possible that certain cancerous tissues express elevated levels of this Uev1 splice variant. Such a condition could lead to up-regulation of growth promoting proteins such as EGFR and ultimately to an adverse effect on controlling growth of the cells.

Supplementary Material

Refer to Web version on PubMed Central for supplementary material.

Acknowledgments

We thank Drs. Timothy Thomson, Stanley Lin, Wei Xiao, Harald Stenmark, Ira Mellman and George Banting for providing us with cDNA constructs and antibodies. We also thank Lai Kuan Goh and Melissa Adams for help in preparation of the manuscript. J.E.D. was supported by a NCI/NRSA (F32CA126344) fellowship and A.S. is supported by a grant from NCI (CA089151).

References

1. Sorkin A, Goh LK. Endocytosis and intracellular trafficking of ErbBs. Exp Cell Res 2009;315:683–96. [PubMed: 19278030]
2. Hicke L, Dunn R. Regulation of membrane protein transport by ubiquitin and ubiquitin-binding proteins. Annu Rev Cell Dev Biol 2003;19:141–72. [PubMed: 14570567]
3. Raiborg C, Rusten TE, Stenmark H. Protein sorting into multivesicular endosomes. Curr Opin Cell Biol 2003;15:446–55. [PubMed: 12892785]
4. Alwan HA, van Leeuwen JE. UBPY-mediated epidermal growth factor receptor (EGFR) de-ubiquitination promotes EGFR degradation. J Biol Chem 2007;282:1658–69. [PubMed: 17121848]
5. Bowers K, Piper SC, Edeling MA, Gray SR, Owen DJ, Lehner PJ, Luzio JP. Degradation of endocytosed epidermal growth factor and virally ubiquitinated major histocompatibility complex class I is independent of mammalian ESCRTII. J Biol Chem 2006;281:5094–105. [PubMed: 16371348]
6. McCullough J, Clague MJ, Urbe S. AMSH is an endosome-associated ubiquitin isopeptidase. J Cell Biol 2004;166:487–92. [PubMed: 15314065]
7. Mizuno E, Iura T, Mukai A, Yoshimori T, Kitamura N, Komada M. Regulation of epidermal growth factor receptor down-regulation by UBPY-mediated deubiquitination at endosomes. Mol Biol Cell 2005;16:5163–74. [PubMed: 16120644]
8. Niendorf S, Oksche A, Kisser A, Lohler J, Prinz M, Schorle H, Feller S, Lewitzky M, Horak I, Knobeloch KP. Essential role of ubiquitin-specific protease 8 for receptor tyrosine kinase stability and endocytic trafficking in vivo. Mol Cell Biol 2007;27:5029–39. [PubMed: 17452457]
9. Row PE, Prior IA, McCullough J, Clague MJ, Urbe S. The ubiquitin isopeptidase UBPY regulates endosomal ubiquitin dynamics and is essential for receptor down-regulation. J Biol Chem. 2006
10. Hasdemir B, Murphy JE, Cottrell GS, Bunnett NW. Endosomal deubiquitinating enzymes control ubiquitination and down-regulation of proteaseactivated receptor 2. J Biol Chem 2009;284:28453–66. [PubMed: 19684015]
11. Kim MS, Kim JA, Song HK, Jeon H. STAM-AMSH interaction facilitates the deubiquitination activity in the C-terminal AMSH. Biochem Biophys Res Commun 2006;351:612–8. [PubMed: 17078930]
12. Row PE, Liu H, Hayes S, Welchman R, Charalabous P, Hofmann K, Clague MJ, Sanderson CM, Urbe S. The MIT domain of UBPY constitutes a CHMP binding and endosomal localization signal required for efficient epidermal growth factor receptor degradation. J Biol Chem 2007;282:30929–37. [PubMed: 17711858]
13. Aoh QL, Castle AM, Hubbard CH, Katsumata O, Castle JD. SCAMP3 negatively regulates epidermal growth factor receptor degradation and promotes receptor recycling. Mol Biol Cell 2009;20:1816–32. [PubMed: 19158374]
14. Roxrud I, Raiborg C, Pedersen NM, Stang E, Stenmark H. An endosomally localized isoform of Eps15 interacts with Hrs to mediate degradation of epidermal growth factor receptor. J Cell Biol 2008;180:1205–18. [PubMed: 18362181]
15. Sorkina T, Miranda M, Dionne KR, Hoover BR, Zahniser NR, Sorkin A. RNA interference screen reveals an essential role of Nedd4-2 in dopamine transporter ubiquitination and endocytosis. J Neurosci 2006;26:8195–205. [PubMed: 16885233]
16. Duex JE, Sorkin A. RNA interference screen identifies Usp18 as a regulator of epidermal growth factor receptor synthesis. Mol Biol Cell 2009;20:1833–44. [PubMed: 19158387]
17. Sancho E, Vila MR, Sanchez-Pulido L, Lozano JJ, Paciucci R, Nadal M, Fox M, Harvey C, Bercovich B, Loukili N, Ciechanover A, Lin SL, Sanz F, Estivill X, Valencia A, Thomson TM. Role of UEV-1, an inactive variant of the E2 ubiquitin-conjugating enzymes, in in vitro differentiation and cell cycle behavior of HT-29-M6 intestinal mucosecretory cells. Mol Cell Biol 1998;18:576–89. [PubMed: 9418904]
18. Andersen PL, Zhou H, Pastushok L, Moraes T, McKenna S, Ziola B, Ellison MJ, Dixit VM, Xiao W. Distinct regulation of Ubc13 functions by the two ubiquitin-conjugating enzyme variants Mms2 and Uev1A. J Cell Biol 2005;170:745–55. [PubMed: 16129784]

19. Xiao W, Lin SL, Broomfield S, Chow BL, Wei YF. The products of the yeast MMS2 and two human homologs (hMMS2 and CROC-1) define a structurally and functionally conserved Ubc-like protein family. Nucleic Acids Res 1998;26:3908–14. [PubMed: 9705497]
20. Tebar F, Bohlander SK, Sorkin A. Clathrin assembly lymphoid myeloid leukemia (CALM) protein: localization in endocytic-coated pits, interactions with clathrin, and the impact of overexpression on clathrin-mediated traffic. Mol Biol Cell 1999;10:2687–702. [PubMed: 10436022]
21. Galperin E, Verkhusha VV, Sorkin A. Three-chromophore FRET microscopy to analyze multiprotein interactions in living cells. Nat Methods 2004;1:209–17. [PubMed: 15782196]
22. Sorkina T, Doolen S, Galperin E, Zahniser NR, Sorkin A. Oligomerization of dopamine transporters visualized in living cells by fluorescence resonance energy transfer microscopy. J Biol Chem 2003;278:28274–83. [PubMed: 12746456]
23. Sorkin A, McClure M, Huang F, Carter R. Interaction of EGF receptor and grb2 in living cells visualized by fluorescence resonance energy transfer (FRET) microscopy. Curr Biol 2000;10:1395–8. [PubMed: 11084343]
24. Frederick BA, Helfrich BA, Coldren CD, Zheng D, Chan D, Bunn PA Jr, Raben D. Epithelial to mesenchymal transition predicts gefitinib resistance in cell lines of head and neck squamous cell carcinoma and non-small cell lung carcinoma. Mol Cancer Ther 2007;6:1683–91. [PubMed: 17541031]
25. Hofmann RM, Pickart CM. Noncanonical MMS2-encoded ubiquitin-conjugating enzyme functions in assembly of novel polyubiquitin chains for DNA repair. Cell 1999;96:645–53. [PubMed: 10089880]
26. McKenna S, Spyracopoulos L, Moraes T, Pastushok L, Ptak C, Xiao W, Ellison MJ. Noncovalent interaction between ubiquitin and the human DNA repair protein Mms2 is required for Ubc13-mediated polyubiquitination. J Biol Chem 2001;276:40120–6. [PubMed: 11504715]
27. Rothofsky ML, Lin SL. CROC-1 encodes a protein which mediates transcriptional activation of the human FOS promoter. Gene 1997;195:141–9. [PubMed: 9305758]
28. Thomson TM, Lozano JJ, Loukili N, Carrio R, Serras F, Cormand B, Valeri M, Diaz VM, Abril J, Burset M, Merino J, Macaya A, Corominas M, Guigo R. Fusion of the human gene for the polyubiquitination coeffector UEV1 with Kua, a newly identified gene. Genome Res 2000;10:1743–56. [PubMed: 11076860]
29. Sorkin AD, Teslenko LV, Nikolsky NN. The endocytosis of epidermal growth factor in A431 cells: a pH of microenvironment and the dynamics of receptor complex dissociation. Exp Cell Res 1988;175:192–205. [PubMed: 2894318]
30. Chin LS, Raynor MC, Wei X, Chen HQ, Li L. Hrs interacts with sorting nexin 1 and regulates degradation of epidermal growth factor receptor. J Biol Chem 2001;276:7069–78. [PubMed: 11110793]
31. Lu Q, Hope LW, Brasch M, Reinhard C, Cohen SN. TSG101 interaction with HRS mediates endosomal trafficking and receptor down-regulation. Proc Natl Acad Sci U S A 2003;100:7626–31. [PubMed: 12802020]
32. Morino C, Kato M, Yamamoto A, Mizuno E, Hayakawa A, Komada M, Kitamura N. A role for Hrs in endosomal sorting of ligand-stimulated and unstimulated epidermal growth factor receptor. Exp Cell Res 2004;297:380–91. [PubMed: 15212941]
33. Urbe S, Sachse M, Row PE, Preisinger C, Barr FA, Strous G, Klumperman J, Clague MJ. The UIM domain of Hrs couples receptor sorting to vesicle formation. J Cell Sci 2003;116:4169–79. [PubMed: 12953068]
34. Miranda M, Wu CC, Sorkina T, Korstjens DR, Sorkin A. Enhanced ubiquitylation and accelerated degradation of the dopamine transporter mediated by protein kinase C. J Biol Chem 2005;280:35617–24. [PubMed: 16109712]
35. Pornillos O, Alam SL, Rich RL, Myszka DG, Davis DR, Sundquist WI. Structure and functional interactions of the Tsg101 UEV domain. Embo J 2002;21:2397–406. [PubMed: 12006492]
36. Sundquist WI, Schubert HL, Kelly BN, Hill GC, Holton JM, Hill CP. Ubiquitin recognition by the human TSG101 protein. Mol Cell 2004;13:783–9. [PubMed: 15053872]
37. Bonifacino JS, Traub LM. Signals for sorting of transmembrane proteins to endosomes and lysosomes. Annu Rev Biochem 2003;72:395–447. [PubMed: 12651740]

38. Liu X, Brodeur SR, Gish G, Songyang Z, Cantley LC, Laudano AP, Pawson T. Regulation of c-Src tyrosine kinase activity by the Src SH2 domain. Oncogene 1993;8:1119–26. [PubMed: 7683128]
39. O'Brien KB, Argetsinger LS, Diakonova M, Carter-Su C. YXXL motifs in SH2-Bbeta are phosphorylated by JAK2, JAK1, and platelet-derived growth factor receptor and are required for membrane ruffling. J Biol Chem 2003;278:11970–8. [PubMed: 12551917]
40. Songyang Z, Shoelson SE, Chaudhuri M, Gish G, Pawson T, Haser WG, King F, Roberts T, Ratnofsky S, Lechleider RJ, et al. SH2 domains recognize specific phosphopeptide sequences. Cell 1993;72:767–78. [PubMed: 7680959]
41. Bache KG, Brech A, Mehlum A, Stenmark H. Hrs regulates multivesicular body formation via ESCRT recruitment to endosomes. J Cell Biol 2003;162:435–42. [PubMed: 12900395]
42. Raiborg C, Bache KG, Mehlum A, Stang E, Stenmark H. Hrs recruits clathrin to early endosomes. Embo J 2001;20:5008–21. [PubMed: 11532964]
43. Belleudi F, Leone L, Maggio M, Torrisi MR. Hrs regulates the endocytic sorting of the fibroblast growth factor receptor 2b. Exp Cell Res 2009;315:2181–91. [PubMed: 19362549]
44. Ma L, Broomfield S, Lavery C, Lin SL, Xiao W, Bacchetti S. Up-regulation of CIR1/CROC1 expression upon cell immortalization and in tumor-derived human cell lines. Oncogene 1998;17:1321–6. [PubMed: 9771976]
45. Ito M, Shichijo S, Tsuda N, Ochi M, Harashima N, Saito N, Itoh K. Molecular basis of T cell-mediated recognition of pancreatic cancer cells. Cancer Res 2001;61:2038–46. [PubMed: 11280764]

Abbreviations

Uev1	ubiquitin E2 variant
EGFR	epidermal growth factor receptor
ESCRT	endosomal sorting complex required for transport
Hrs	Hepatocyte growth factor regulated tyrosine kinase substrate

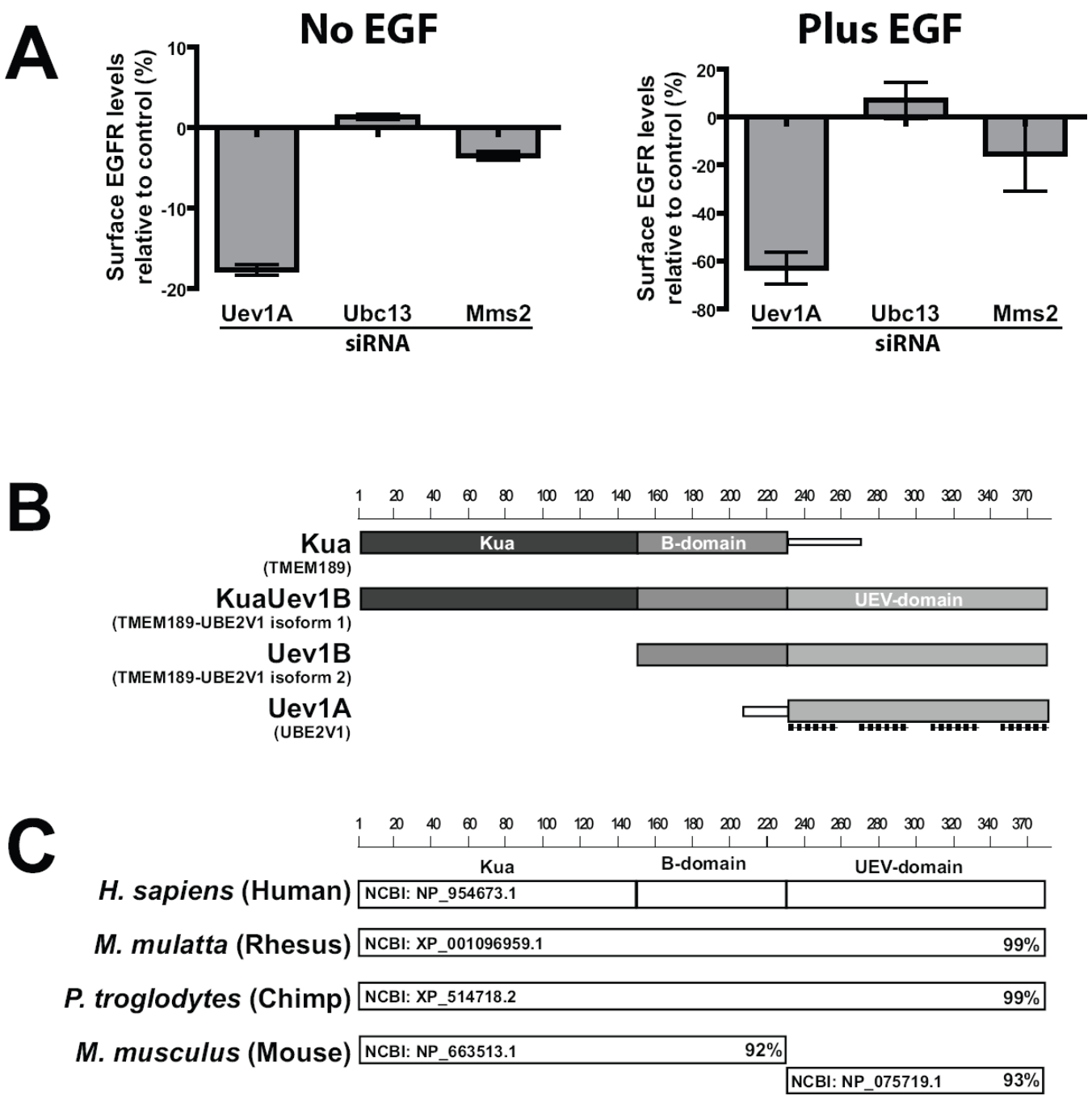

Figure 1. Treatment of cells with siRNA targeting Uev1A promotes EGFR down-regulation

(A) SCC2 cells underwent reverse siRNA transfection (75 nM) for 72 hrs. These cells were then untreated or treated with 100 ng/ml EGF for 4 hrs followed by fixation. The cell surface levels of EGFR were quantitated using an “in cell western” technique as described in “Methods”. The surface levels of EGFR from cells treated with targeting siRNAs were normalized to surface levels of EGFR from control cells treated with non-targeting siRNA. The values are plotted as the percent change from control (set to zero) with negative numbers representing a decrease in surface levels of EGFR. Data is representative of three independent experiments.

(B) Diagram showing the four different protein products that can be generated from the human Uev1 gene locus. Alternative protein names are shown in parentheses. The shaded boxes represent conserved domains and are 100% identical between the different proteins shown here. Also shown are the target sites of the four individual siRNA oligonucleotides (dashed lines) targeting Uev1A. Scale represents number of amino acids.
(C) BLAST analysis of the human KuaUev1B protein reveals orthologs in rhesus and chimpanzee protein databases. The KuaUev1B protein does not have a single mouse ortholog but rather two proteins which have near identity to the human KuaUev1B protein. The NCBI protein accession number is displayed to the left while the percent identity to human KuaUev1B is displayed on the right.

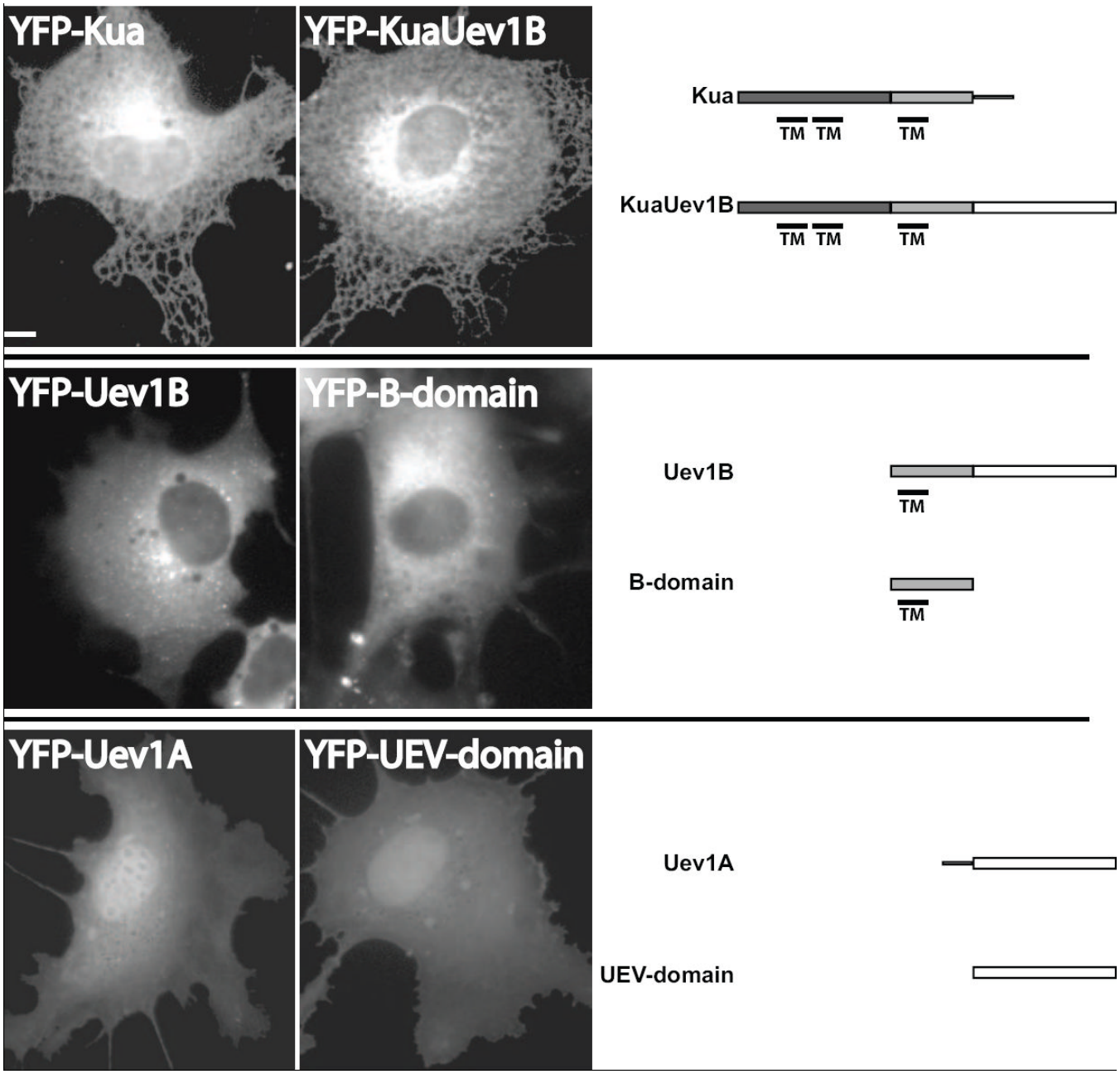

Figure 2. Cellular distribution of the Uev1 locus proteins differs dramatically

COS1 cells were transfected with YFP-fusion constructs of the indicated protein or conserved domain. The cells were imaged after 48 hrs. The predicted transmembrane domains (TM) are shown below each protein profile and were determined consistently between SOSUI (Nagoya University, Japan), TMHMM Server v2.0 (Technical University of Denmark, Denmark), and TMpred (Swiss EMBnet). Scale bar, 10μm.

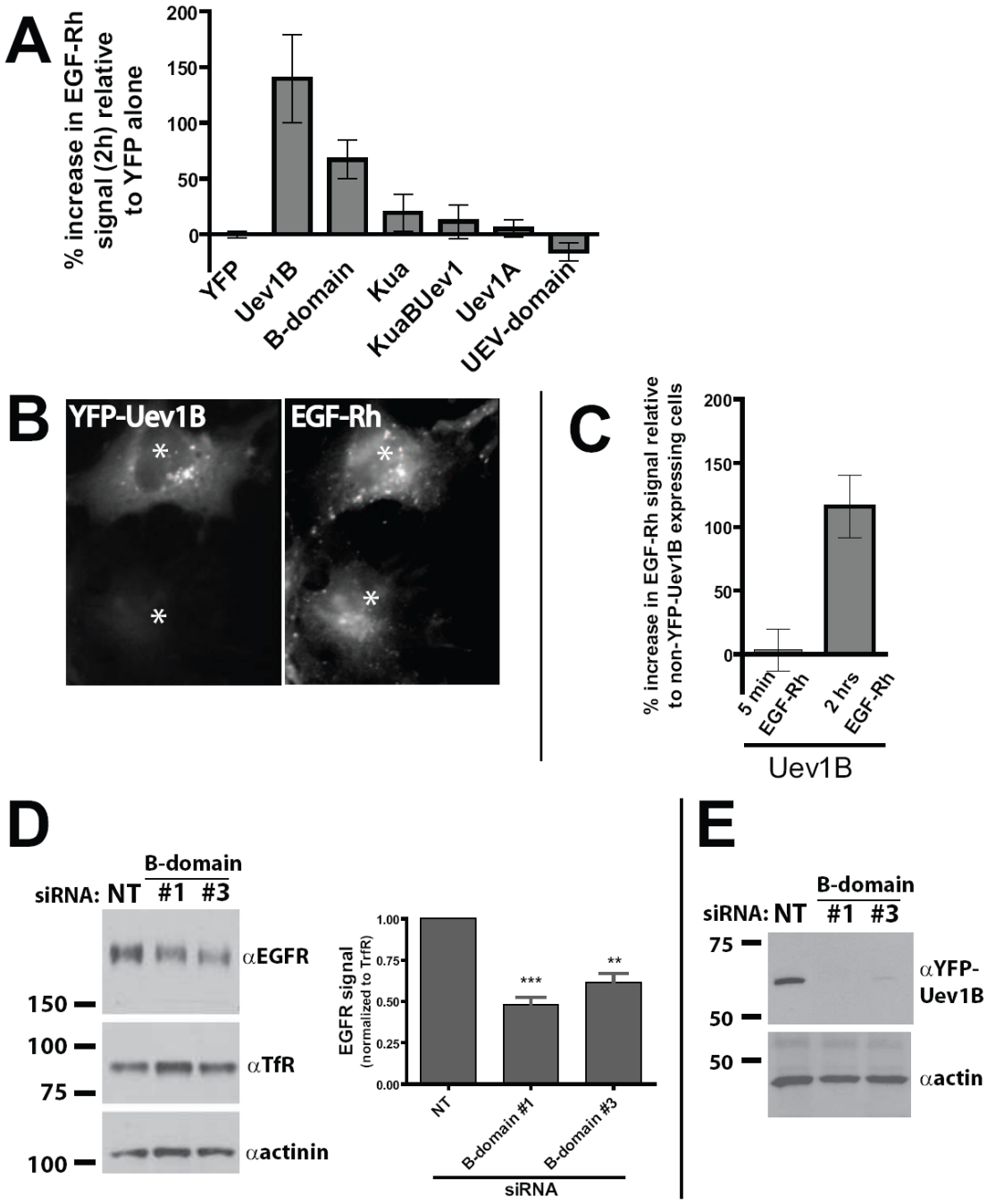

Figure 3. Overexpression of Uev1B inhibits degradation of EGFR:ligand complexes while RNAi against Uev1B promotes degradation of EGFR

(A) COS1 cells were transfected with YFP-fusions of the Uev1 locus proteins. After 48 hrs the cells were pulse-labeled with EGF-Rh for 45 min at 4°C followed by a 2 hr chase at 37°C. Fixed cells were then imaged by acquiring 20-stack z-series, and the EGF-Rh signal was quantitated for individual cells. The percent increase in EGF-Rh signal is the EGF-Rh signal from cells expressing a YFP-fusion over the EGF-Rh signal from cells on the same coverslip which exhibited no YFP signal. The percent increases were then normalized so that the YFP alone condition is zero. A minimum of 30 cells were quantitated for each condition over three independent experiments.

(B) A representative image demonstrating the high level of EGF-Rh signal remaining in COS1 cells overexpressing YFP-Uev1B relative to untransfected cells.
(C) COS1 cells were transfected with YFP-Uev1B or YFP alone and pulse-labeled with EGF-Rh as in (A). Cells were then chased at 37°C for either 5 min or 2 hrs before fixation and EGF-Rh quantitation. For each time point EGF-Rh signal in Uev1B overexpressing cells is shown as a percent increase from EGF-Rh signal in non-YFP expressing cells. A minimum of 10 cells were quantitated over two independent experiments.
(D) Blots from a representative experiment in which SCC2 cells were treated with two different siRNA oligonucleotides targeting the B-domain of Uev1B. After 72 hours the levels of EGFR and transferrin receptor (TfR) were analyzed by western blot. The graph shows data from 5 independent experiments in which EGFR levels were normalized to TfR levels. The EGFR signal from Uev1B siRNA treated cells is displayed as a percentage of EGFR signal from non-targeting (NT) siRNA treated cells. *** denotes $p < 0.0005$ NT vs. #1; ** denotes $p < 0.005$ NT vs. #3.
(E) Representative blot showing that the Uev1B siRNA oligonucleotides completely block expression of YFP-Uev1B while NT siRNA does not. COS1 cells were treated with siRNA and 24 hrs later cells were transfected with both pYFP-Uev1B and siRNA. After an additional 24 hrs YFP-Uev1B expression was analyzed by SDS-PAGE and western blot.

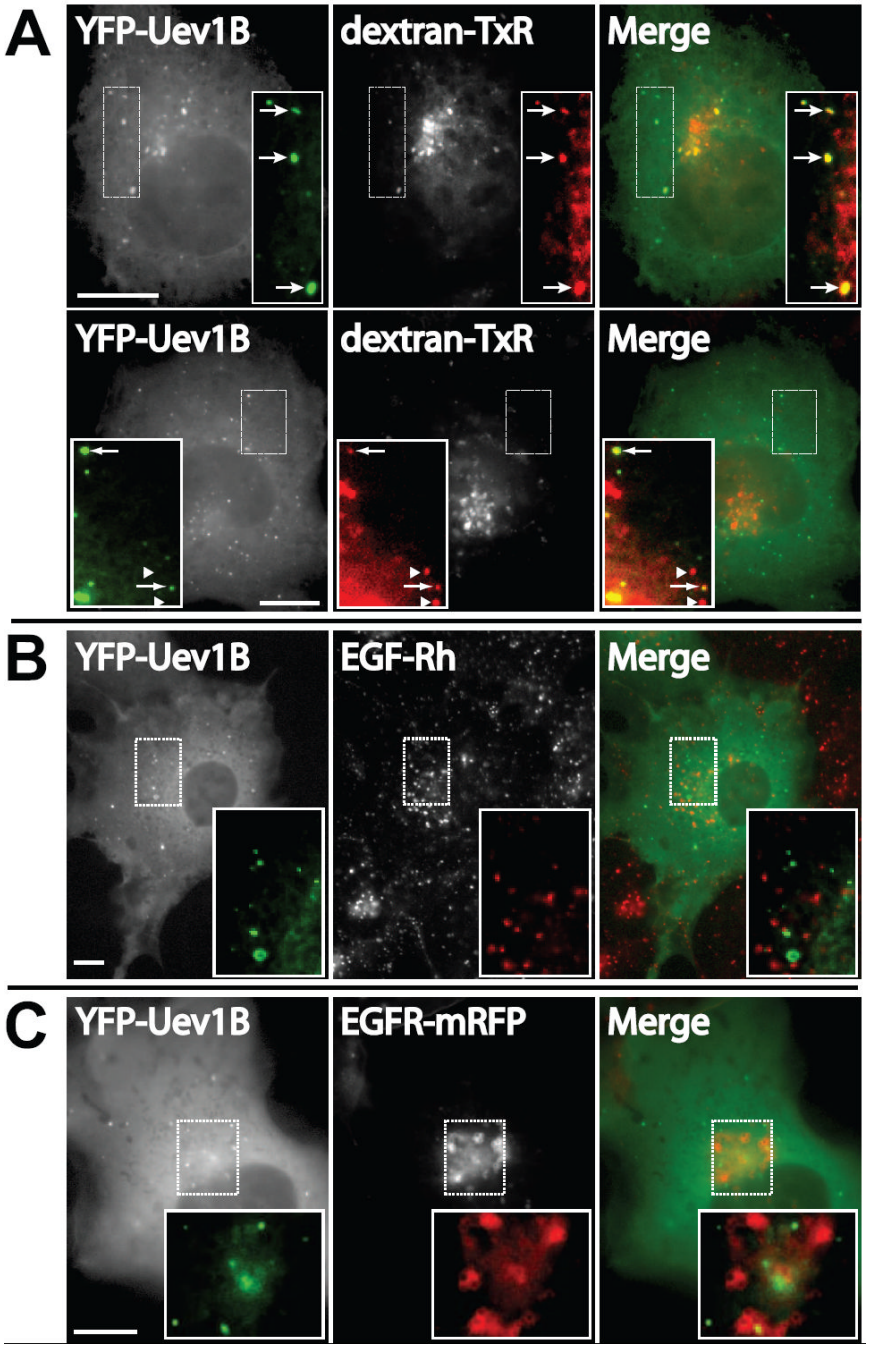

Figure 4. Overexpressed Uev1B colocalizes with internalized dextran but not with internalized EGFR or its ligand

(A) YFP-Uev1B was overexpressed in COS1 cells for 48 hrs followed by pulse-labeling with dextran-Texas-Red (dextran-TxR) for 15 min at 37°C followed by a chase of 2 hrs at room temperature. Cells were then fixed and imaged. Two representative images are shown indicating the variation in colocalization.

(B)YFP-Uev1B was overexpressed in COS1 cells for 48 hrs followed by incubation with EGF-Rh for 15 min. The cells were fixed and imaged.

(C) YFP-Uev1B and EGFR-mRFP were co-transfected in COS1 cells for 48 hrs. The cells were then incubated with 40 ng/ml EGF for 15 min followed by fixation and microscopy. Representative images are shown. Scale bars, 10μm.

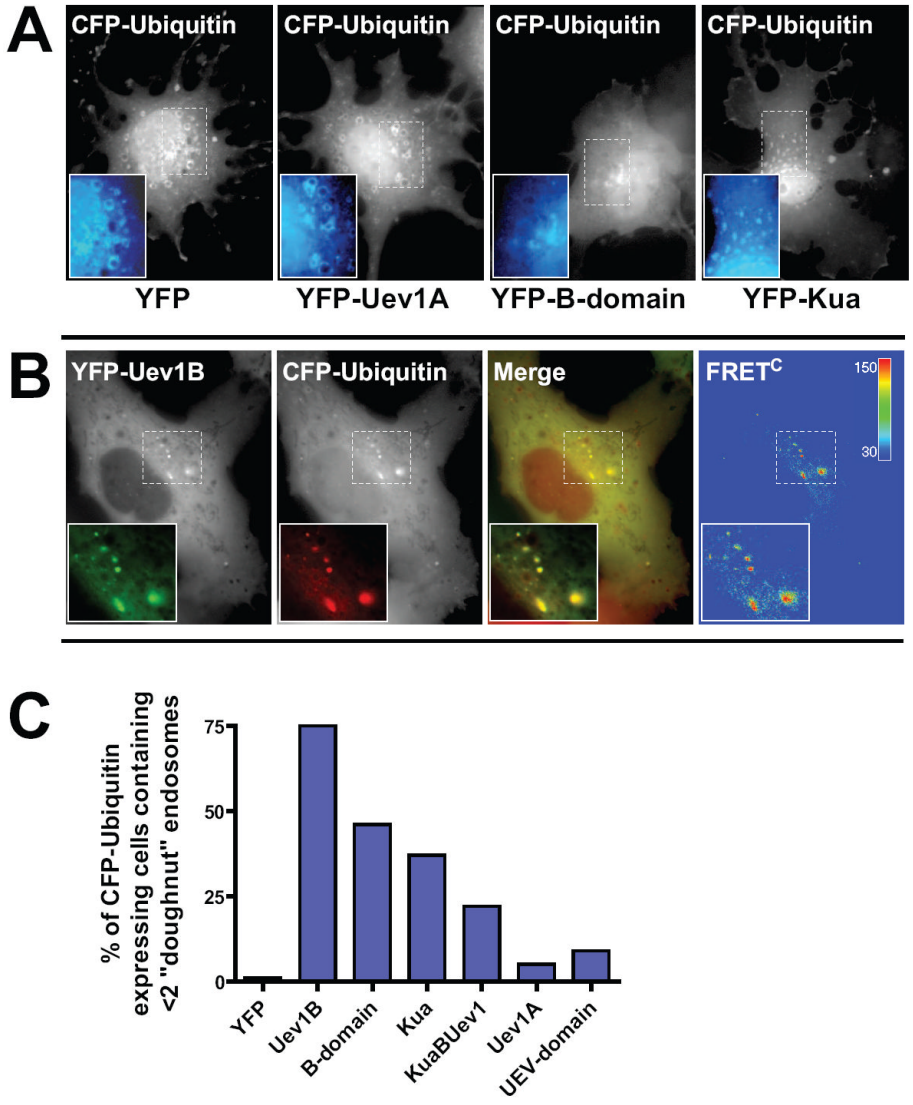

Figure 5. Uev1B overexpression suppresses the "enlarged-endosome" phenotype induced by elevated CFP-ubiquitin levels

(A) COS1 cells were co-transfected with CFP-Ubiquitin and either YFP alone or various other YFP-fusion constructs as indicated. After 48 hrs the cells were fixed and imaged. Representative CFP-Ubiquitin images are shown.

(B) For cells transfected with YFP-Uev1B FRET channel images were also acquired. For purposes of merging the images the YFP channel was pseudo-colored green while the CFP channel was pseudo-colored red. Corrected $FRET^C$ images were generated as described in "Methods". Significant $FRET^C$ was observed for at least 25 cells.

(C) Cells co-expressing CFP-ubiquitin and YFP-fusion proteins as in (A) were visually analyzed for endosome morphology. Cells were scored as either having two or fewer large "doughnut-shaped" endosomes or more than two of these large endosomes. A minimum of 104 cells were analyzed for each condition from three independent experiments.

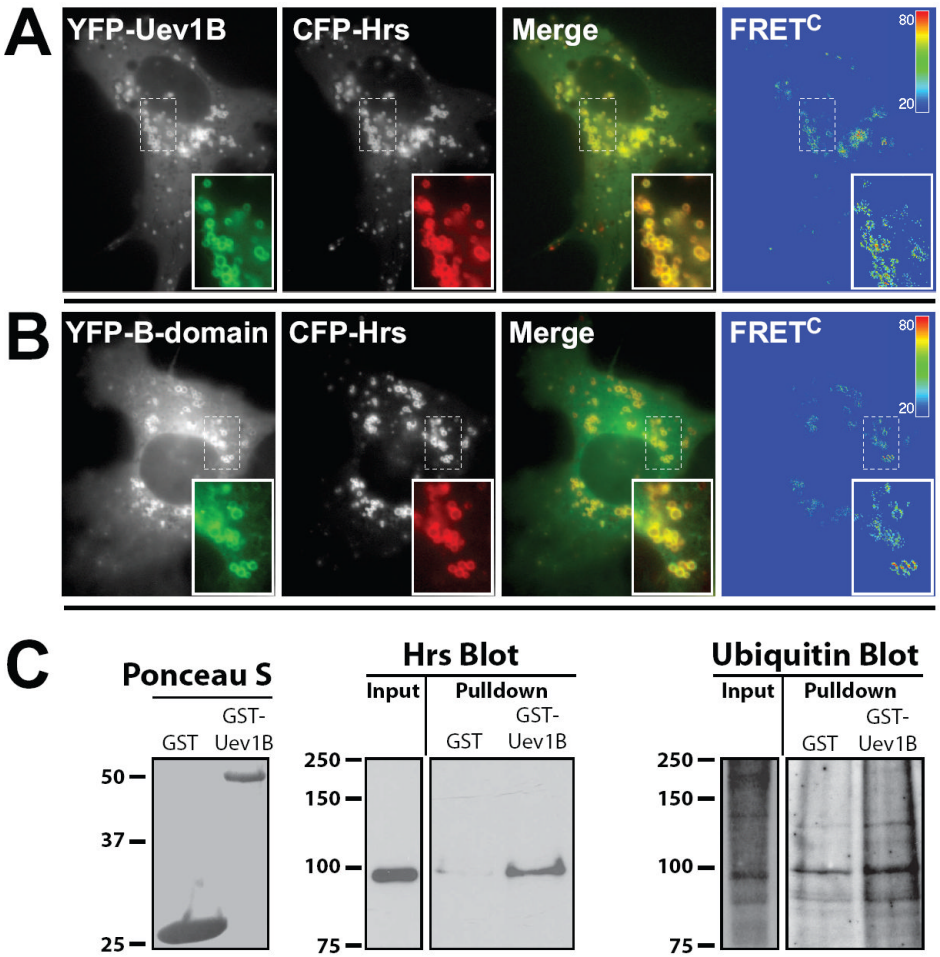

Figure 6. Uev1B associates with Hrs whose overexpression results in the recruitment of Uev1B to endosomes

(A) COS1 cells were co-transfected with YFP-Uev1B and CFP-Hrs. After 48 hrs the cells were fixed and imaged, including FRET channel capture. Images are displayed and processed as described in Figure 5.

(B) The same approach as in (A) but using a YFP-B-domain instead of YFP-Uev1B construct. Images are representative of at least 3 independent experiments. Significant $FRET^C$ was observed for at least 14 cells.

(C) Recombinant Uev1B was purified from bacteria and subsequently incubated with HeLa cell extracts. Precipitated proteins were washed and subjected to SDS-PAGE followed by western blot analysis. Relative to control protein Uev1B is able to pull-down Hrs and ubiquitinated proteins from cellular extracts.

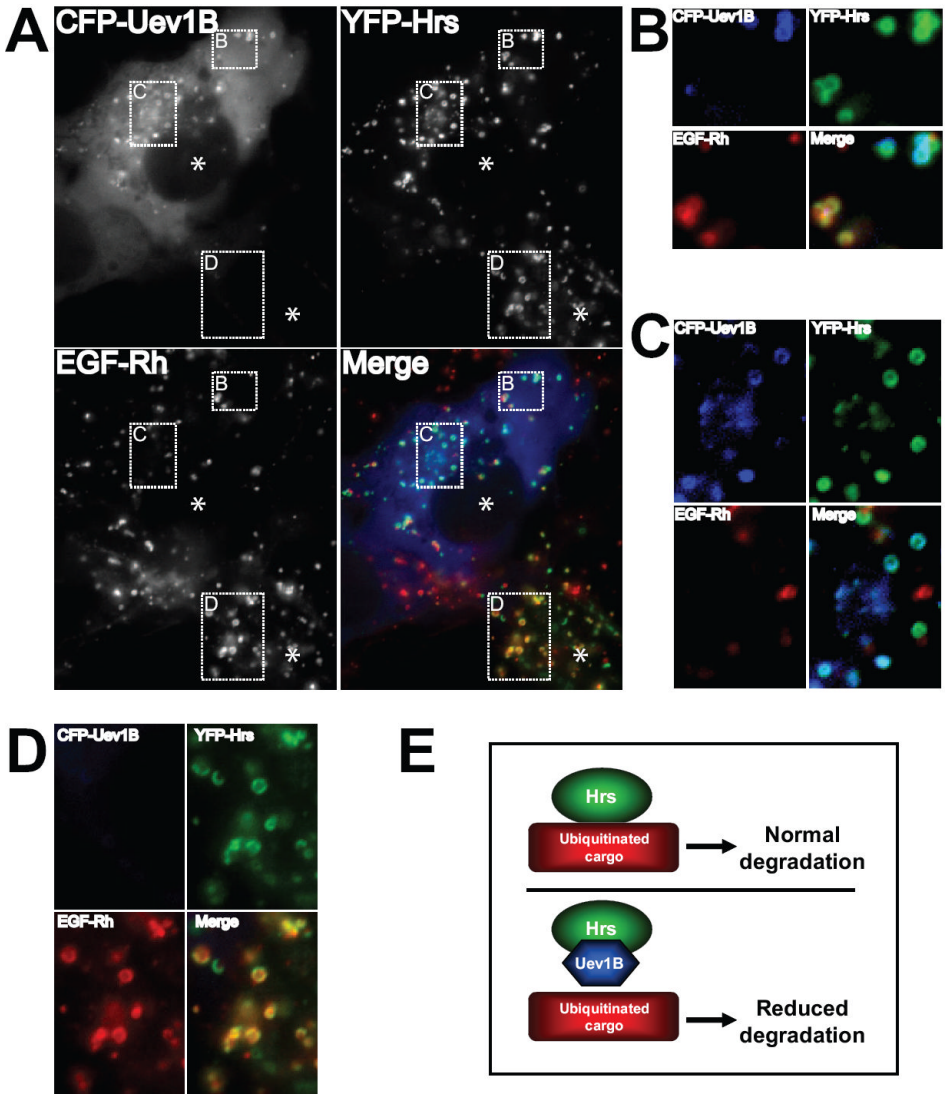

Figure 7. The presence of Uev1B precludes Hrs association with internalized EGF-Rh

(A) COS1 cells were transfected with CFP-Uev1B or YFP-Hrs. After 48 hrs the cells were treated with 40 ng/ml EGF-Rh for 20 min, fixed and imaged. A representative image is presented showing one cell expressing CFP-Uev1B and YFP-Hrs while the other cell in the same field is only expressing YFP-Hrs. The CFP channel was pseudo-colored blue, the YFP channel was pseudo-colored green, and the Rhodamine channel was pseudo-colored red.

(B and C) High-magnification of the region of the cell showing that Uev1B positive endosomes contain Hrs but are largely devoid of EGF-Rh, while Uev1B negative endosomes contain both Hrs and EGF-Rh.

(D) High magnification of the region of a cell not expressing Uev1B showing that nearly all Hrs signal colocalizes with EGF-Rh signal.

(E) Simplified model suggesting that elevated levels of Uev1B competitively associate with Hrs and thus inhibit the efficient sorting of ubiquitinated cargo for degradation.